JULY 14 2025

Methods for predicting overall sound power and maximum overall sound pressure levels from heated supersonic jets, including rockets

Logan T. Mathews ; Kent L. Gee

J. Acoust. Soc. Am. 158, 371–379 (2025)
https://doi.org/10.1121/10.0037192

JASA ARTICLE

Methods for predicting overall sound power and maximum overall sound pressure levels from heated supersonic jets, including rockets

Logan T. Mathews[a] and Kent L. Gee[b]
Department of Physics and Astronomy, Brigham Young University, Provo, Utah 84602, USA

ABSTRACT:
Prior work [e.g., McInerny (1992). Noise Control Eng. J. **38**(1), 5–16; McInerny (1996). J. Aircraft **33**(3), 511–517; Franken (1958). Noise Control **4**(3), 8–16] has resulted in models for estimating overall sound power levels (OAPWLs) and maximum overall sound pressure levels ($OASPL_{max}$) from jet and rocket engines. Based on fundamental flow properties, this paper builds on previous results and presents simple methods for predicting OAPWL and $OASPL_{max}$ from heated supersonic jets and rockets. A method for estimating ground effects on $OASPL_{max}$ is also presented. The model's performance is evaluated for launched Atlas V and Vulcan Centaur rockets and an installed F404 jet engine at engine conditions ranging from 38% thrust through afterburner. The results show good agreement for $OASPL_{max}$, where the root mean square error is confined to less than 2 dB for the rockets and jet engine conditions considered. © *2025 Acoustical Society of America*.
https://doi.org/10.1121/10.0037192
(Received 29 March 2025; revised 6 June 2025; accepted 26 June 2025; published online 14 July 2025)
[Editor: Con Doolan] Pages: 371–379

I. INTRODUCTION

Numerous models exist for predicting the far-field radiated noise from supersonic jets and rockets. These models range from simple computations that can be performed on a scientific calculator to full-featured prediction suites, complete with graphical interfaces, that compute advanced noise metrics. Although the complex noise prediction software packages are appealing and useful, elementary models still retain merit. In particular, when fast, reasonably accurate basic metrics are needed, such models excel at providing predictions. Additionally, if these models are based on fundamental flow parameters, they can serve as a straightforward link between flow properties and noise characteristics. Such capabilities may be useful in noise reduction efforts. Furthermore, many advanced models build on the same methodologies as this simple model, such as calculating sound power and, hence, may benefit from advances in these computations.

More advanced models, such as "RUMBLE" (Bradley *et al.*, 2018) and "RNOISE" (Sutherland, 1993; Plotkin *et al.*, 2004; Plotkin, 2010) for rockets, and the Advanced Acoustic model (AAM; Page *et al.*, 2009), Aircraft NOise Prediction Program (ANOPP; NASA Langley Research Center, 2010), and the SAE ARP876F standard (SAE International, 2021) for jets provide advanced metrics, such as sound exposure levels with various weightings, and include numerous model inputs such as weather information and detailed vehicle trajectory. Whereas complex models such as these have great utility in community noise and environmental impact assessments, basic models such as that in this paper provide a quick, simple way to predict basic acoustic parameters. Additionally, advanced noise models do not always produce accurate results (Gee *et al.*, 2024), hence, further research into modeling is warranted.

This paper builds on similar models established by Franken (1958), Franken (1960), and McInerny (1996) by expanding into elementary flow parameters and adding a dedicated correction for ground effects for observers near the ground. Additionally, this model broadens its scope to supersonic air jets and rockets, as the aforementioned models focused on only one application regime. This model for maximum overall sound pressure levels ($OASPL_{max}$) is validated against modern, high-fidelity acoustic data from launched rockets and a full-scale installed jet engine. Because the methods presented in this paper form the basis for several widely used empirical noise models—such as NASA SP-8072 (Eldred, 1971) and its derivatives (e.g., Lubert *et al.*, 2022), "RUMBLE" and "RNOISE"—the discussion provided here is directly relevant to those models as well.

II. MODEL

Here, the predictive methodology is given in two main parts. First, overall sound power level (OAPWL) is estimated from elementary flow parameters. Second, $OASPL_{max}$ is calculated. A correction for ground effects is then outlined. Finally, the effects of using exit vs fully-expanded (FE) parameters for computing the overall sound power are quantified.

[a]Email: loganmathews@byu.edu
[b]Email: kentgee@byu.edu

A. OAPWL

To begin, the jet mechanical stream power, W_m, is expressed as

$$W_m = \frac{1}{2} F U_e \tag{1}$$

(Franken, 1958; Sutton and Biblarz, 2017; Walter, 2019), where F is the total jet thrust and U_e is the mean jet velocity at the nozzle exit. Thrust can be written in terms of jet and ambient fluid properties as

$$F = \dot{m}_e U_e + (P_e - P_0) A_e = \left[\rho_e U_e^2 + (P_e - P_0)\right] A_e \tag{2}$$

(Mattingly, 2006; Sutton and Biblarz, 2017), where $\dot{m}_e$ is the mass flow rate at the nozzle exit, P_e is the mean pressure at the nozzle exit, P_0 is the ambient pressure, A_e is the nozzle exit area, and ρ_e is the mean density at the nozzle exit. The first term, $\dot{m}_e U_e$, is known as the momentum thrust, and the second term, $(P_e - P_0)A_e$, is the pressure thrust. In the case of an ideally expanded jet, $P_e = P_0$, and the pressure thrust term goes to zero, leaving only the momentum thrust term. However, even when the jet is operating at imperfectly expanded conditions, the pressure thrust term is still relatively small (further quantification of this is provided in Sec. II D). Hence, the pressure thrust term is often discarded, and thrust is approximated as

$$F \approx \dot{m}_e U_e = \rho_e U_e^2 A_e. \tag{3}$$

Substituting this expression back into Eq. (1), the approximate mechanical power in terms of elementary flow properties is given as

$$W_m \approx \frac{1}{2} \rho_e U_e^3 A_e. \tag{4}$$

With the mechanical power defined, an acoustic efficiency parameter $\eta = W_a / W_m$ is introduced to relate the mechanical and acoustic powers (Lighthill, 1952), where W_a is the acoustic power. Historically, the acoustic efficiency of supersonic jets and rockets has been bounded in the range $0.1\% < \eta < 1\%$ (Eldred, 1971; Lubert *et al.*, 2022). Using the efficiency, the overall acoustic power can be given as

$$W_a = \eta W_m \approx \frac{1}{2} \eta \rho_e U_e^3 A_e = \frac{\pi}{8} \eta \rho_e U_e^3 D_e^2, \tag{5}$$

where D_e is the exit diameter, written in this form for convenience as diameter is often used instead of area. Because total acoustic power is typically formatted as a decibel quantity as the OAPWL, Eq. (5) is equivalent to

$$\begin{aligned} \mathrm{OAPWL} &= 10 \log_{10}\left(\frac{W_a}{W_{\mathrm{ref}}}\right) \approx 10 \log_{10}\left(\frac{\pi}{8 W_{\mathrm{ref}}} \eta \rho_e U_e^3 D_e^2\right) \\ &= 115.9 + 10 \log_{10}\left(\eta \rho_e U_e^3 D_e^2\right) \ \mathrm{dB}. \end{aligned} \tag{6}$$

This constitutes a compact formulation for calculating the overall acoustic power from elementary flow parameters. Given the simplicity of Eq. (6), it may be useful in applications that pursue optimizing/minimizing the acoustic power of a supersonic jet; as OAPWL is expressed in terms of these fundamental flow properties, it may be possible to determine which parameters can be altered to reduce the total jet sound power output while preserving thrust.

If the pressure thrust term is non-negligible, such as may be the case for significantly over- or underexpanded jets, OAPWL can be more accurately expressed as

$$\begin{aligned} \mathrm{OAPWL} = 115.9 + 10 \log_{10}\big(\eta U_e D_e^2 \big[\rho_e U_e^2 \\ + (P_e - P_0)\big]\big) \ \mathrm{dB}. \end{aligned} \tag{7}$$

In applications in which the thrust is known and density is unknown, it may be more useful to express OAWPL in terms of thrust, using Eq. (1), such that

$$\begin{aligned} \mathrm{OAPWL} &= 10 \log_{10}\left(\frac{W_a}{W_{\mathrm{ref}}}\right) \\ &= 117.0 + 10 \log_{10}(\eta F U_e) \ \mathrm{dB}. \end{aligned} \tag{8}$$

B. Maximum overall sound pressure level ($\mathrm{OASPL_{max}}$)

From the OAPWL, overall sound pressure levels (OASPLs) can then be estimated. This is performed by considering the source to be compact and directional. Whereas the aeroacoustic source of a jet is distributed, in the far-field, its behavior can be approximated as a simple source. Yet, how does the noise amplitude decay with distance? SP-8072 (Eldred, 1971) assumes spherical decay, as do McInerny (1996), Franken (1958), and Franken (1960). Given the shock-like content of supersonic jet and rocket noise waveforms, the noise amplitude decay can be bounded by spherical spreading and weak shock theory, which specify pressure amplitude decay rates of r^{-1} and $r^{-1}(\ln r)^{-1/2}$ (Blackstock *et al.*, 2024), respectively. Here, spherical spreading is considered; however, certain applications may benefit from adjustments to the decay rate, although it should be noted that a different spatial decay rate may modify the apparent acoustic efficiency and directivity index. For spherical spreading, the expression for OASPL at an observer point (r, θ, ϕ) is written as

$$\begin{aligned} \mathrm{OASPL}(r, \theta, \phi) \approx \mathrm{OAPWL} - 10 \log_{10}(4\pi r^2) \\ + Q_{\mathrm{OA}}(\theta, \phi), \end{aligned} \tag{9}$$

where r is the distance from the source to the receiver, θ is the angle between the source-to-receiver vector and the jet plume direction, ϕ is the source-to-receiver vector azimuthal angle, and $Q_{\mathrm{OA}}(\theta, \phi)$ are the overall source directivity indices. Although this calculation assumes spherical spreading from the source $(4\pi r^2)$, note that some models, such as those by Franken (1958) and Franken (1960), instead, implement hemispherical spreading $(2\pi r^2)$ to

https://doi.org/10.1121/10.0037192

account for a horizontally oriented jet on the ground plane, which is approximated as a half-space problem with incoherent ground reflections.

Jets and rockets are typically modeled as azimuthally symmetric sources, particularly when a single nozzle or tightly clustered nozzles are used. Under this assumption, the directivity index varies only with polar angle θ, denoted as $Q_{\mathrm{OA}}(\theta)$. Although modern rockets are often approximated as azimuthally symmetric, azimuthal asymmetries in jet and rocket noise remain an active area of research. Directivity indices can be measured experimentally or obtained from empirical models (Eldred, 1971; James *et al.*, 2014; Hart *et al.*, 2023). Whereas OASPL as a function of θ provides insight into the angular variation of noise, it is common practice to focus on the maximum directivity angle, $\theta_{\max}$, to characterize maximum overall sound levels. This metric is widely used in jet and rocket noise literature as a first-order indicator of maximum acoustic loading and commonly referenced in environmental assessments. In such cases, the directivity index can be simplified to its maximum value, $Q_{\max,\mathrm{OA}} = Q_{\mathrm{OA}}(\theta_{\max})$. Accordingly, the expression for $\mathrm{OASPL}_{\max}$ of an azimuthally symmetric source is given by

$$\mathrm{OASPL}_{\max}(r) \approx \mathrm{OAPWL} - 10\log_{10}(4\pi r^2) + Q_{\max,\mathrm{OA}}. \tag{10}$$

C. Ground effects

The expressions presented thus far for $\mathrm{OASPL}_{\max}$ assume a free-space problem with no ground effects. However, most observers in a jet noise problem will be located near a finite-impedance ground surface. Thus, in addition to the sound transmitted to the receiver directly, there will also be reflected sound that reaches the observer. The ground effect on the sound pressure level at the receiver is complicated and involves ray-path geometry, ground impedance, and noise frequency.

For a medium- to large-sized rocket, the peak frequency is typically quite low with most sound energy being constrained to frequencies below 40 Hz. Hart and Gee (2023) discussed the effect of reflections from a finite-impedance ground surface for rocket launches with observers near the ground. Their findings indicated that for most common surfaces (e.g., dirt, grass, and pavement), the ground would increase $\mathrm{OASPL}_{\max}$ by 5.5–6 dB relative to free-field conditions for rockets with a peak frequency < 60 Hz. This corresponds to $\mathrm{OASPL}_{\max}$ increasing by a factor of 1.9–2. This simplified method of accounting for ground effects uses a parameter δ that can be included in the model as

$$\mathrm{OASPL}_{\max}(r) \approx \mathrm{OAPWL} - 10\log_{10}(4\pi r^2) + Q_{\max,\mathrm{OA}} + 20\log_{10}(\delta), \tag{11}$$

where $\delta = 1$ for the free-space $\mathrm{OASPL}_{\max}$ and $\delta = 2$ for observers on a rigid ground surface. For higher frequency signals, such as jet aircraft engines (peak frequencies between 80 and 500 Hz depending on engine and operating condition), or for lower-impedance ground surfaces (such as soft snow), the factor may be less. For instance, Christian *et al.* (2023a) implemented a ground reflection model for a full-scale static jet measurement and elevated microphones over hard-packed dirt; their results indicate $1.7 < \delta < 1.2$ for a range of engine conditions, where the fully supersonic engine conditions are $1.2 < \delta < 1.3$. However, these were obtained for elevated microphones placed at 1.5 m above ground level. If comparing to ground-based measurements, δ will generally approach two. To this end, the sonic boom community has long used a ground reflection factor of 1.9 for ground-based measurements (Onyeowu, 1975).

To provide an estimation for values of δ, the methodology of Hart and Gee (2023) is followed here, with a few caveats. Instead of modeling the rocket noise spectrum as a simple "haystack" shape, this analysis uses a spectral shape with a broader peak, which is more representative of measured rocket noise. This was achieved by using a modified version of the empirical formula associated with noise from large-scale turbulence structures by Tam *et al.* (1996). Discussion of this modified empirical spectrum is given in Appendix A. The model of Embleton *et al.* (1983) is used to estimate the spectral ground effects at various values of effective flow resistivities. Figure 1(a) shows an example model spectrum with a peak frequency of 30 Hz (an upper bound for medium-lift class rockets) and three estimated, ground-affected spectra corresponding to ground surfaces with different effective flow resistivities (σ, in units of cgs rayls), each with receiver heights of 6 mm. For reference, $\sigma = 20$ corresponds to soft snow, $\sigma = 200$ corresponds to grass, and $\sigma = 100\,000$ corresponds to concrete (Embleton *et al.*, 1983). The effect on the OASPL of each spectrum and the correction factor, δ, are also displayed. Figure 1(b) shows the calculated values of δ for a wide range of spectral peak frequencies and values of σ. These values were computed assuming a receiver height of 6 mm.

D. Exit vs FE parameters

An important distinction to make is whether to use exit or equivalent FE jet parameters when estimating sound power. Some models specify which parameter to use, whereas others remain agnostic. Exact thrust and mechanical calculations, such as those in Eq. (2), employ exit parameters. However, in many situations, the parameters for the pressure thrust term are unknown and, hence, some have advocated for using FE parameters instead, which would not require the inclusion of pressure thrust (e.g., Varnier, 2001). Although it is impossible to quantify the difference between using exit and FE parameters for all jets, in general, the degree to which the difference will matter depends on the specific jet operating parameters—the closer to ideally expanded that a jet is, the less the difference between exit and FE parameters will be. As noted by Lubert *et al.* (2022), the question of whether to use exit or FE parameters remains unresolved. Therefore, a practical comparison of thrust and mechanical power calculated using both sets of parameters is presented here.

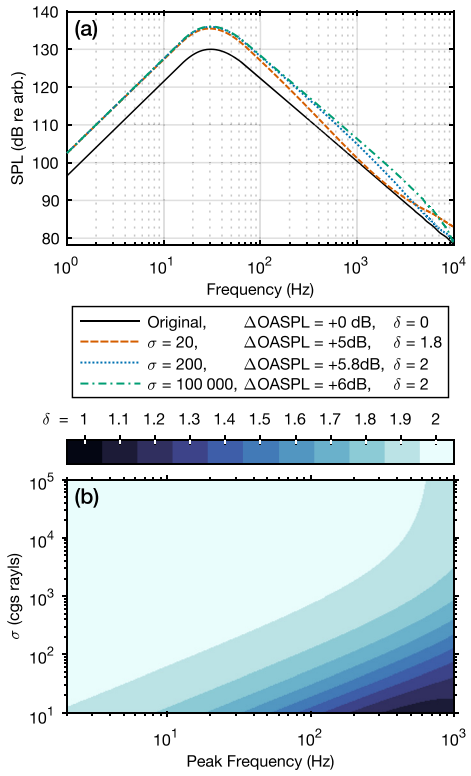

FIG. 1. (a) Sample spectrum with modeled ground effects for an observer 6 mm above the ground at three representative values of σ, and (b) estimated values of δ calculated for model spectra of varying peak frequencies and values of σ are shown.

To quantify the differences between exit and FE power calculations, Table I shows the difference for an afterburning military jet engine and several rockets. The estimation of parameters used in this analysis is discussed in Appendix B. In terms of thrust, the most accurate estimate is given using Eq. (2) with exit parameters. Using FE in place of exit parameters in Eq. (2) also yields accurate results. However, neglecting the pressure thrust term with exit conditions, as is the case with the simplified Eq. (3), yields appreciable thrust errors for the F404 engine at the two lowest engine powers but not for the rocket engines that are considered. It should be noted that these two lower engine conditions for the F404 are in the transonic regime.

In terms of mechanical (and acoustic) power, using the exact expressions of Eqs. (1) and (2) is accurate to within 0.1 dB for all engines and conditions. Aside from the 38% and 55% thrust conditions for the T-7A, the error in mechanical power for the approximate Eq. (4) with either exit for FE parameters is accurate to within 0.3 dB. Hence, whereas we recommend using the full equations with exit parameters whenever feasible, using approximated expressions for calculating the mechanical/acoustic power with either exit or FE parameters yields reasonable results, particularly for rockets.

E. Meteorological and propagation effects

Meteorological conditions can significantly influence noise propagation from jets and rockets, especially at greater distances from the source. Atmospheric absorption, wind, and refractive effects, such as curved-ray propagation, can all contribute to variability in received noise levels. Additionally, nonlinear propagation phenomena may further affect the acoustic signatures observed at far-field locations. Given the complexity and site-specific nature of these effects, a comprehensive treatment is beyond the scope of this work. However, the predictive model developed here can be used in conjunction with corrections from established propagation models—such as ray-tracing techniques and nonlinear acoustic models—which can be used to improve far-field accuracy when such refinements are needed.

III. VALIDATION

In the following examples, the models for OAPWL [Eqs. (6) and (7)] and $\mathrm{OASPL_{max}}$ [Eq. (11)] are validated for two types of supersonic jets: launched, medium-lift class rockets and a high-performance afterburner-capable jet engine. These two scenarios are representative of the types of applications this model is designed for.

A. Rockets

To validate the model for rockets, the predicted $\mathrm{OASPL_{max}}$ values are compared to those obtained through measurements from two liquid-fueled Atlas V 401 rocket launches from Space Launch Complex-3E (SLC-3E) at Vandenberg Space Force (VSFB), CA. Launch details and surface weather conditions for each launch are given in

TABLE I. Error in thrust and mechanical power calculated using exit conditions (exact and without pressure thrust terms), as well as with FE parameters for the F404 jet engine and Merlin 1D, RD-180, and BE-4 rocket engines.

			Thrust error (%)			Mechanical power error (dB)		
Vehicle	Engine	Condition	Eq. (2)	Eq. (3)	Eq. (2), FE	Eqs. (1) and (2)	Eq. (4)	Eq. (4), FE
T-7A	F404	38% thrust	0%	48%	3%	0.0	1.7	−1.4
T-7A	F404	55% thrust	1%	32%	2%	0.0	1.2	−1
T-7A	F404	MIL	1%	8%	1%	0.1	0.4	−0.3
T-7A	F404	AB	2%	11%	1%	0.1	0.4	−0.3
Falcon 9	Merlin 1D	100% thrust	1%	3%	0%	0.0	0.1	−0.1
Atlas V	RD-180	100% thrust	0%	4%	1%	0.0	0.2	−0.1
Vulcan/New Glenn	BE-4	100% thrust	1%	6%	3%	0.1	0.3	−0.1

https://doi.org/10.1121/10.0037192

TABLE II. Launch details and surface weather information for the three launches considered.

Vehicle and mission	Launch site	Launch date/ time (UTC)	Weather observation time	Temperature (°C)	Relative humidity (%)	Wind speed (m/s)	Wind direction (deg)	Cloud cover
Atlas V Landsat 9	VSFB, SLC-3E	27 Sep 2021, 18:12	L + 0:19	15	88	2.6	330	Overcast
Atlas V JPSS-2	VSFB, SLC-3E	10 Nov 2022, 09:49	L − 0:01	8	76	2.1	70	Clear
VC Cert-2	CCSFS, SLC-41	04 Oct 2024, 11:25	L + 0:00	27	87	1	104	Scattered

Table II. Further details for the Atlas V Landsat 9 and JPSS-2 launches are given by Cunningham *et al.* (2023) and Mathews *et al.* (2023), respectively. Furthermore, the model is validated against a recent measurement of the Vulcan Centaur (VC) Cert-2 launch from Space Launch Complex-41 (SLC-41) at Cape Canaveral Space Force Station (CCSFS), FL. This rocket used liquid engines and solid rocket motors. OASPL values were computed from measured waveforms using 1-s blocks with 50% overlap. For the model input parameters, estimations were made from publicly available data and computational tools, which is discussed in Appendix B and are reported in Table III. The acoustic efficiency is assumed to be $\eta = 0.33\%$ per the findings of Kellison and Gee (2023). To account for ground effects, a value of $\delta = 1.9$ is chosen based on Fig. 1, given the measurements were largely made on either dirt or a vegetated surface, and the rocket peak frequencies are <30 Hz. $Q_{\max,\mathrm{OA}}$ is chosen to be 5 dB, based on the findings of McInerny (1996), although it should be noted that this parameter deserves more study. Notably, McInerny (1996) used $Q_{\max,\mathrm{OA}}$ values of 5 dB to estimate average levels across the 6 dB re maximum region and 8 dB for estimating maximum 1-s block averaged $\mathrm{OASPL}_{\max}$ values. However, ground effects were not separately accounted for in the model by McInerny (1996). When accounting for ground effects separately, such as in Eq. (11), $Q_{\max,\mathrm{OA}}$ reduces from 8 to 5 dB.[1]

The resulting predictions, compared with measured values, are reported in Fig. 2 as a function of approximate distance from the source. This distance is approximated by assuming a nominal maximum emission angle of 71° for the Atlas V based on the findings of Mathews *et al.* (2021) for the Falcon 9,[2] as the RD-180 engines of the Atlas V use the same propellant as and have similar performance to the Merlin 1D engines of Falcon 9. Furthermore, a recently proposed convective Mach number model by Gee *et al.* (2025) estimates the peak directivity angle as $\theta_{\max} \approx \cos^{-1}[(c_0/U_e)^{1/2}]$, which also yields $\theta_{\max} \approx 71°$. For the VC vehicle, this is somewhat more complicated as there are two types of engines. Following the methods of Kellison *et al.* (2024) for the Space Launch System rocket, another vehicle with liquid engines and solid rocket motors, a maximum emission angle is estimated to be 69° for the VC2 configuration. The resulting predictions for $\mathrm{OASPL}_{\max}$ from the Atlas V launches in Fig. 2(a) shows good agreement, generally, where the root mean square error (RMSE) is confined to less than 1.8 dB between measurement and prediction.

Interestingly, Fig. 2(a) shows two different data trends, which are grouped by launch. The JPSS-2 launch fits the linear, spherical decay rate (r^{-1}, –20 dB/decade) of Eq. (11) well. However, the Landsat 9 $\mathrm{OASPL}_{\max}$ values appear to decay faster. As mentioned in Sec. II B, weak shock theory would predict a decay rate of $r^{-1}(\ln r)^{-1/2}$ (Blackstock *et al.*, 2024). In the far-field, this approximates to $r^{-1.1}$ (–22 dB/decade; ANSI/ASA, 2011), which is indicated by the gray dashed line. It appears that the Landsat 9 $\mathrm{OASPL}_{\max}$ values follow this decay rate. Although a thorough investigation into the cause of this discrepancy is beyond the scope of this paper, one hypothesis is proposed here. At the respective launches, the surface weather conditions indicated 15 °C/88% relative humidity (RH) and 8 °C/76% RH for Landsat 9 and JPSS-2, respectively. Additionally, the Landsat 9 launch had overcast conditions with dense fog, whereas the JPSS-2 launch was clear. The increased atmospheric humidity at ground level and in the atmosphere at the Landsat 9 launch would decrease absorption (ANSI/ASA, 2009), leading to more shock-like waveforms that would decay closer to weak shock theory.

For the VC Cert-2 launch, depicted in Fig. 2(b), a different trend emerges. Using the same values of η, $Q_{\max,\mathrm{OA}}$, and δ reveals a general overprediction of measured values by 3 dB, which is indicated by the solid line. However, if η is halved (resulting in an acoustic efficiency of 0.17%), the fit is substantially improved with a RMSE of 1.7 dB. This suggests that the acoustic efficiency of the VC2 vehicle is lower than that of the Atlas V 401. One postulate for this discrepancy is that the separated plumes of the VC2 vehicle result in a lower acoustic efficiency than the tightly clustered plumes of the Atlas V 401. Further research is necessary to establish the cause of this apparent difference in acoustic efficiency between these two vehicles.

TABLE III. Estimated plume parameters for the Atlas V 401 and VC VC2 rockets.

Vehicle	Engine/motor	Number	Component total		Vehicle total	
			F (MN)	W_m (GW)	F (MN)	W_m (GW)
Atlas V 401	RD-180	1	3.83	6.06	3.83	6.06
VC VC2	BE-4	2	4.90	7.80	9.02	12.9
	GEM 63XL	2	4.12	5.09		

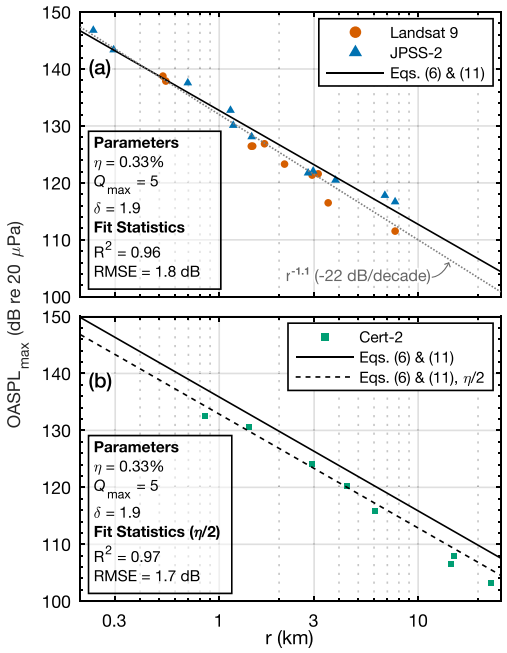

FIG. 2. (a) $OASPL_{max}$ as measured for two different Atlas V launches compared to predictions via Eqs. (6) and (11), and (b) $OASPL_{max}$ for a VC launch compared to predictions via Eqs. (6) and (11) for two different values of acoustic efficiency are shown.

B. Full-scale, afterburner-capable jet engine

To extend the validation regime beyond rockets, the model is applied to the GE F404, a full-scale jet engine capable of afterburning operation. The data are from a 2019 measurement of the T-7A trainer aircraft, details of which can be found in Leete *et al.* (2021). The model is applied at four different operating conditions: 38% thrust, 56% thrust, MIL ("military" power, 100% non-afterburning thrust), and maximum afterburner (AB, 152% thrust). As reported by Christian *et al.* (2023a), the FE Mach numbers at these conditions are 0.94, 1.1, 1.43, and 1.46, hence, the data represent engine conditions ranging from transonic to supersonic.

As more detailed jet parameters are available for this application (see Appendix B), the full, pressure thrust-inclusive model of Eqs. (7) and (11) is used and compared to the approximated, pressure thrust neglecting model, consisting of Eqs. (6) and (11). Additionally, condition-specific model parameters are used, which are shown in Table IV. Values for η are from the results of Christian *et al.* (2023b) and values of δ are determined from the ground reflection correction results at each engine condition's peak directivity angle by Christian *et al.* (2023a). Q_{max} values are determined from a refined methodology of Christian *et al.* (2022). The primary reasons for δ values being lower than the rocket example in Sec. III A are that the peak frequencies are significantly higher (100–500 Hz), and the jet measurements were made 1.5 m off the ground.

The jet parameters are used to compare the model against data measured at elevated microphones. Figure 3(a) shows the measurement locations for each engine condition analyzed here. These locations are chosen to align with the peak directivity angle at each engine condition, as specified by Gee *et al.* (2025). The measured and predicted $OASPL_{max}$ for the four engine conditions at various distances are shown in Fig. 3(b). Markers indicate the average $OASPL_{max}$ values for all six engine runups while bars indicate the measurement $OASPL_{max}$ variability across the runups. Notably, the spread in measured $OASPL_{max}$, particularly at greater propagation distances, is substantial—showing variability of up to ±3 dB from the mean. Streeter *et al.* (2024) investigated this variability and attributed it primarily to changes in meteorological conditions during the measurement period. Engine conditions were reproduced with high accuracy, exhibiting expected thrust variations of less than 0.5%.[3] Because the observed variability increases with propagation distance, meteorological factors are the most likely source of the differences. Comparing to the

TABLE IV. Values of parameters η, Q_{max}, and δ used for the T-7A/F404 engine at the four engine conditions.

Engine condition	η	Q_{max}	δ
38% Thrust	0.014%	7.4 dB	1.68
56% Thrust	0.19%	7.5 dB	1.23
MIL (100% thrust)	0.51%	7.0 dB	1.21
AB (152% thrust)	0.61%	5.9 dB	1.29

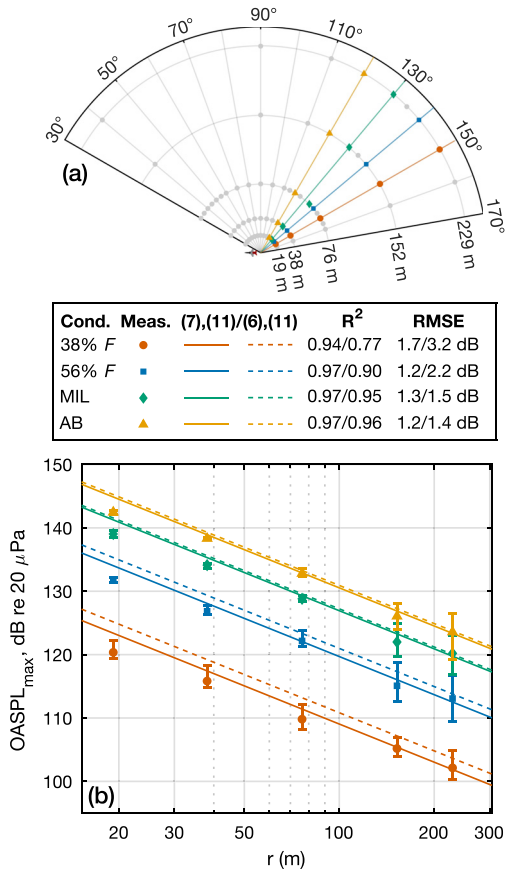

FIG. 3. (a) Measurement locations for peak directivity angles at four T-7A/F404 engine conditions, (b) measured $OASPL_{max}$ compared to predictions at four T-7A/F404 engine conditions with full [Eqs. (7) and (11)] and approximated [Eqs. (6) and (11)] models are shown. Markers indicate the average $OASPL_{max}$ values for all six engine runups while bars indicate the measurement $OASPL_{max}$ variability across the runups.

https://doi.org/10.1121/10.0037192

measurements, the full model for $OASPL_{max}$, consisting of Eqs. (7) and (11), shows excellent agreement across all engine conditions with RMSE < 1.7 dB. When the lowest engine condition is excluded, the RMSE improves to <1.3 dB. For each engine condition, the near-field measurements at 19 m appear to be outliers. The approximated expressions, consisting of Eqs. (6) and (11), are less accurate, particularly for the two lowest engine conditions, with the RMSE growing to 3.2 dB at the lowest condition. However, at MIL and AB, the RMSE for the approximate model is less than 1.5 dB.

IV. CONCLUSION

Models for overall sound power and maximum overall sound pressure levels from supersonic heated supersonic jets, such as jet engines and rockets, have been formulated and demonstrated. A simple method for accounting for near-ground effects is outlined, based on a model spectrum designed to replicate the spectral shapes of supersonic jet noise and rocket noise in the peak radiation direction. The effects of neglecting pressure thrust and those using FE jet parameters instead of exit parameters are quantified for a jet engine at various operating conditions, as well as for several rockets.

The model predicts measured maximum sound levels well for three launched rockets and an installed jet engine at four operating powers, with a RMSE generally less than 2 dB. Different apparent decay rates in maximum overall sound pressure levels are observed between two launches of the same rocket type, indicating possible differences caused by atmospheric conditions. It is noted that to accurately predict the levels for the VC Cert-2 launch, the acoustic efficiency used in the model must be a factor of 2 less than that for the Atlas V 401 vehicle, assuming the maximum overall directivity indices are the same. To improve this and other modeling approaches, further research into the acoustic efficiencies, maximum overall directivity indices, and spatial noise decay rates of jets and rockets are warranted.

ACKNOWLEDGMENTS

The authors thank Mark C. Anderson for his measurements of the VC rocket used in this study. This research was supported in part by the appointment of L.T.M. and Mark C. Anderson to the Department of Defense (DOD) Research Participation Program administered by the Oak Ridge Institute for Science and Education (ORISE) through an interagency agreement between the U.S. Department of Energy (DOE) and the DOD. ORISE is managed by Oak Ridge Associated Universities (ORAU) under DOE Contract No. DE-SC0014664. All opinions expressed in this paper are those of the authors and do not necessarily reflect the policies and views of DOD, DOE, or ORAU/ORISE. The authors acknowledge the Office of Naval Research for funding the T-7A analysis under Grant No. N00014-21-1-2069 with project monitor Steven Martens, Code 351 Jet Noise Reduction. The T-7A measurements were funded through the Advanced Pilot Training System Program Office and Air Force Research Laboratory. The Atlas V measurements were supported in part by Vandenberg Space Force Base through the United States Army Corps of Engineers. Space Launch Delta 30 at Vandenberg Space Force Base is acknowledged for logistical support. Distribution Statement A, approved for public release; distribution unlimited, cleared 28 March 2025.

AUTHOR DECLARATIONS

Conflict of Interest

The authors have no conflicts to disclose.

DATA AVAILABILITY

The data that support the findings of this study are available from the United States Department of Defense (United States Air Force/Space Force/Navy). Restrictions apply to the availability of these data, which were used under license for this study. Data are available from the authors upon reasonable request and with the permission of the United States Department of Defense (United States Air Force/Space Force/Navy).

APPENDIX A: MODEL SPECTRA

To estimate ground effects on measured spectra, a model spectrum was constructed. This was achieved empirically by modifying the large-scale turbulence similarity spectra of Tam *et al.* (1996). Although this similarity spectrum is widely applied in jet noise, Lubert *et al.* (2022) discuss that the spectral shape disagrees with measured spectra at peak radiation angles from supersonic jets and rockets, particularly the high-frequency slope. To this end, the large-scale similarity spectrum equation from Tam *et al.* (1996) is modified here to have a low-frequency slope of $f^{2.5}$ (25 dB/decade) and a high-frequency slope of $f^{-2.2}$ (–22 dB/decade) to approximate the spectral shapes of supersonic jets and rockets. This modified equation is given as

$$S(f,f_{pk}) = \begin{cases} 3.82974 - 22\log_{10}\left(\frac{f}{f_{pk}}\right) & \text{if } \frac{f}{f_{pk}} \geq 2.5, \\ \left[1.06617 - 42.2994\log_{10}\left(\frac{f}{f_{pk}}\right) + 21.40972\log_{10}\left(\frac{f}{f_{pk}}\right)^2\right], & \\ \log_{10}\left(\frac{f}{f_{pk}}\right) & \text{if } 2.5 > \frac{f}{f_{pk}} \geq 1, \\ -50.19338\log_{10}\left(\frac{f}{f_{pk}}\right)^2, & \\ -16.91175\log_{10}\left(\frac{f}{f_{pk}}\right)^3 & \text{if } 1 > \frac{f}{f_{pk}} \geq 0.5, \\ 3.43861 + 25\log_{10}\left(\frac{f}{f_{pk}}\right) & \text{if } \frac{f}{f_{pk}} < 0.5. \end{cases} \tag{A1}$$

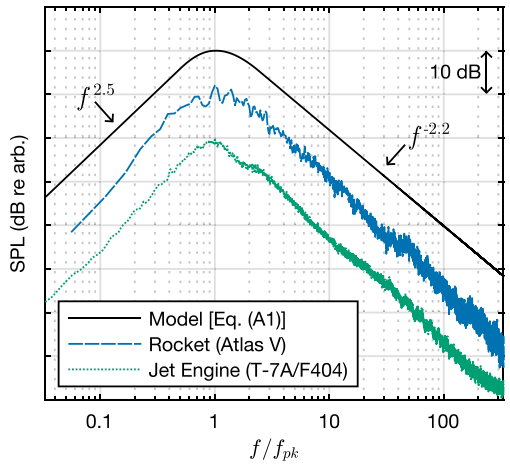

FIG. 4. Model spectrum from Eq. (A1) compared with measured maximum spectra from the Atlas V 401 rocket and the T-7A aircraft at afterburner, normalized relative to the peak frequency, is shown.

This empirical spectral shape is depicted in Fig. 4, alongside representative peak directivity spectra from a launched Atlas V 401 rocket and the T-7A/F404 jet at afterburner. The modified high- and low-frequency slopes closely approximate those of the rocket and supersonic jet engines.

APPENDIX B: JET PARAMETER CALCULATION

Rocket engine parameters are estimated using the NASA CEARUN program (McBride and Gordon, 2004), based on publicly available input parameters for the engines (Katorgin *et al.*, 2004; United Launch Alliance, 2010, 2023). These parameters are summarized in Table V.

Parameters for the GEM 63XL solid rocket motors are based on specifications from Northrop Grumman (2024). The exit velocity for the GEM 63XL motor is estimated from the reported vacuum specific impulse as reported by Northrop Grumman (2024). Given that the exit velocity is expected to differ for a sea-level launch, the exit velocity at launch is estimated by assuming a 10% reduction in specific impulse from vacuum to sea level based on Space Shuttle solid rocket motor performance specifications (Ward, 2010). This gave an approximate sea-level value of $U_e \approx 2.47$ km/s, which is close to that reported for the Space Shuttle solid rocket motor (McInerny, 1992; Ward, 2010).

TABLE V. Input parameters for CEARUN computation of RD-180 and BE-4 engines.

Parameter	RD-180	BE-4
Ambient pressure (kPa)	101.3	101.3
Chamber pressure (MPa)	25.66	13.4
Area ratio	36.87	23.3
Oxidizer/Fuel ratio	2.72	3.5
Fuel	RP-1	CH4(L)
Oxidizer	02(L)	02(L)
Run condition	Frozen, NFZ = 2	Frozen, NFZ = 2

The T-7A/F404 engine parameters were estimated using the Numerical Propulsion System Simulation (NPSS) code (Southwest Research Institute, 2025) using the recorded engine settings from the study and the measured ambient atmospheric conditions.

[1]For a perfectly rigid surface and ground-based observer, $\mathrm{OASPL}_{\max}$ increases by 6 dB and OAPWL increases by 3 dB relative to free-field. Given that $Q_{\max,\mathrm{OA}} = \mathrm{OASPL}_{\max}(r) + 10\log_{10}(4\pi r^2) - \mathrm{OAPWL}$, this means that separately accounting for ground effects results in $Q_{\max,\mathrm{OA}}$ being 3 dB lower than when ground effects are "baked into" the calculation.

[2]Mathews *et al.* (2021) initially found that the maximum directivity angle for the Falcon 9 rocket across three launches was 64°, however, subsequent improvements to their processing code (calculating the true three-dimensional angle to the rocket as opposed to just a two-dimensional approximation) have yielded a more accurate estimation of 71°. The Atlas V 401 and Falcon 9 are propelled by engines using the same fuel/oxidizer mixture, hence, using this result is justified.

[3]In terms of mechanical/acoustic powers, a 0.5% variation in thrust would constitute a 0.02 dB difference, assuming that the exit velocity does not change. Even in a more extreme, worst-case scenario, where the power changes by 5%, this would only result in a difference of 0.2 dB in acoustic output, which is significantly smaller than the variability observed.

ANSI/ASA (**2009**). S1.26-1995, *Calculation of the Absorption of Sound by the Atmosphere* (Acoustical Society of America, New York).
ANSI/ASA (**2011**). S2.20-1983, *Estimating Air Blast Characteristics for Single Point Explosions in Air, with a Guide to Evaluation of Atmospheric Propagation and Effects* (Acoustical Society of America, New York).
Blackstock, D. T., Hamilton, M. F., and Pierce, A. D. (**2024**). "Progressive waves in lossless and lossy fluids," in *Nonlinear Acoustics*, edited by M. F. Hamilton and D. T. Blackstock (Springer, Cham, Switzerland), pp. 63–147.
Bradley, K. A., James, M. M., Salton, A. R., and Boeker, E. R. (**2018**). *Commercial Space Operations Noise and Sonic Boom Modeling and Analysis* (National Academies of Sciences, Engineering, and Medicine Transportation Research Board, Washington, DC).
Christian, M. A., Gee, K. L., Streeter, J. B., Mathews, L. T., Wall, A. T., Johnson, J. P., and Campbell, S. C. (**2022**). "Installed F404 engine noise source characteristics from far-field directivity measurements," in *28th AIAA/CEAS Aeroacoustics Conference*, 14–17 June, Southampton, UK, AIAA Paper 2022–3027.
Christian, M. A., Gee, K. L., Streeter, J. B., Wall, A. T., and Campbell, S. C. (**2023a**). "Implementing a heuristic method to correct ground reflection effects observed in full-scale tactical aircraft noise measurements," Proc. Mtgs. Acoust. **50**(1), 040005.
Christian, M. A., Gee, K. L., Streeter, J. B., Wall, A. T., and Campbell, S. C. (**2023b**). "Sound power and acoustic efficiency of an installed GE F404 jet engine," JASA Express Lett. **3**(7), 073601.
Cunningham, C., Anderson, M. C., Moats, L. T., Gee, K. L., Hart, G. W., and Hall, L. K. (**2023**). "Acoustical measurement and analysis of an Atlas V launch," Proc. Mtgs. Acoust. **46**(1), 045005.
Eldred, K. M. (**1971**). "Acoustic loads generated by the propulsion system," National Aeronautics and Space Administration SP–8072, available at https://ntrs.nasa.gov/citations/20110012036 (Last viewed June 1, 2025).
Embleton, T. F. W., Piercy, J. E., and Daigle, G. A. (**1983**). "Effective flow resistivity of ground surfaces determined by acoustical measurements," J. Acoust. Soc. Am. **74**(4), 1239–1244.
Franken, P. A. (**1958**). "Review of information on jet noise," Noise Control **4**(3), 8–16.
Franken, P. A. (**1960**). "Jet noise," in *Noise Reduction*, edited by L. L. Beranek (McGraw-Hill, New York), pp. 644–666.
Gee, K. L., Olaveson, T. W., and Mathews, L. T. (**2025**). "Convective Mach number and full-scale supersonic jet noise directivity," AIAA J. **63**(4), 1393.
Gee, K. L., Pulsipher, N. L., Kellison, M. S., Mathews, L. T., Anderson, M. C., and Hart, G. W. (**2024**). "Starship super heavy acoustics: Far-field noise measurements during launch and the first-ever booster catch," JASA Express Lett. **4**(11), 113601.

Hart, G. W., and Gee, K. L. (**2023**). "Correcting for ground reflections when measuring overall sound power level and acoustic radiation efficiency of rocket launches," Proc. Mtgs. Acoust. **50**(1), 040004.
Hart, G. W., Gee, K. L., and Cook, M. R. (**2023**). "Corrected frequency-dependent directivity indices for large solid rocket motors," Proc. Mtgs. Acoust. **51**(1), 040007.
James, M. M., Salton, A. R., Gee, K. L., Neilsen, T. B., McInerny, S. A., and Kenny, R. J. (**2014**). "Modification of directivity curves for a rocket noise model," Proc. Mtgs. Acoust. **18**(1), 040008.
Katorgin, B. I., Chvanov, V. K., Chelkis, F. J., Popp, M., Tanner, L. G., van Giessen, R. C., and Connally, S. J. (**2004**). "RD-180 engine production and flight experience," in *40th AIAA/ASME/SAE/ASEE Joint Propulsion Conference and Exhibit*, 11–14 July, Fort Lauderdale, FL, AIAA Paper 2004–3998.
Kellison, M. S., and Gee, K. L. (**2023**). "Sound power of NASA's lunar rockets: Space Launch System versus Saturn V," JASA Express Lett. **3**(11), 113601.
Kellison, M. S., Gee, K. L., Coyle, W. L., Anderson, M. C., Mathews, L. T., and Hart, G. W. (**2024**). "Aeroacoustic analysis of NASA's Space Launch System Artemis-I mission," in *30th AIAA/CEAS Aeroacoustics Conference*, 4–7 June, Rome, Italy, AIAA Paper 2024–3033.
Leete, K. M., Vaughn, A. B., Bassett, M. S., Rasband, R. D., Novakovich, D. J., Gee, K. L., Campbell, S. C., Mobley, F. S., and Wall, A. T. (**2021**). "Jet noise measurements of an installed GE F404 engine," in *AIAA Scitech 2021 Forum*, 11–15 and 19–21 January, virtual event, AIAA Paper 2021–1638.
Lighthill, M. J. (**1952**). "On sound generated aerodynamically I. General theory," Proc. R. Soc. London, Ser. A: Math. Phys. Sci. **211**(1107), 564–587.
Lubert, C. P., Gee, K. L., and Tsutsumi, S. (**2022**). "Supersonic jet noise from launch vehicles: 50 years since NASA SP-8072," J. Acoust. Soc. Am. **151**(2), 752–791.
Mathews, L. T., Anderson, M. C., Gardner, C. D., McLaughlin, B. W., Hinds, B. M., McCullah-Boozer, M. R., Hall, L. K., and Gee, K. L. (**2023**). "An overview of acoustical measurements made of the Atlas V JPSS-2 rocket launch," Proc. Mtgs. Acoust. **51**(1), 040003.
Mathews, L. T., Gee, K. L., and Hart, G. W. (**2021**). "Characterization of Falcon 9 launch vehicle noise from far-field measurements," J. Acoust. Soc. Am. **150**(1), 620–633.
Mattingly, J. D. (**2006**). *Elements of Propulsion: Gas Turbines and Rockets* (American Institute of Aeronautics and Astronautics, Reston, VA).
McBride, B. J., and Gordon, S. (**2004**). "CEARUN," available at https://cearun.grc.nasa.gov/ (Last viewed June 1, 2025).
McInerny, S. A. (**1992**). "Characteristics and predictions of far-field rocket noise," Noise Control Eng. J. **38**(1), 5–16.
McInerny, S. A. (**1996**). "Launch vehicle acoustics. I—Overall levels and spectral characteristics," J. Aircraft **33**(3), 511–517.
NASA Langley Research Center (**2010**). "Aircraft NOise Prediction ProgramExternal," available at https://software.nasa.gov/software/LAR-19861-1 (Last viewed June 1, 2025).
Northrop Grumman (**2024**). "Propulsion products catalog," available at https://www.prd.ngc.agencyq.site/wp-content/uploads/NG-Propulsion-Products-Catalog.pdf (Last viewed June 1, 2025).
Onyeowu, R. O. (**1975**). "Diffraction of sonic boom past the nominal edge of the corridor," J. Acoust. Soc. Am. **58**(2), 326–330.
Page, J. A., Wilmer, C., Schultz, T., Plotkin, K. J., and Czech, J. (**2009**). "Advanced acoustic model technical reference and user manual," Technical Report SERDP Project WP-1304, available at https://apps.dtic.mil/sti/citations/ADA536390 (Last viewed June 1, 2025).
Plotkin, K. J. (**2010**). "A model for the prediction of community noise from launch vehicles," J. Acoust. Soc. Am. **127**(3 Supplement), 1773.
Plotkin, K. J., Sutherland, L. C., and Moudou, M. (**2004**). "Prediction of rocket noise footprints during boost phase," in *3rd AIAA/CEAS Aeroacoustics Conference*, 12–14 May, Atlanta, GA, AIAA Paper 1997–1660.
SAE International (**2021**). "Gas turbine jet exhaust noise prediction," SAE International Standard, available at https://www.sae.org/standards/content/arp876f/ (Last viewed June 1, 2025).
Southwest Research Institute (**2025**). "Numerical Propulsion System Simulation (NPSS)," available at https://software.nasa.gov/software/LAR-19861-1 (Last viewed June 1, 2025).
Streeter, J. B., Olaveson, T. W., Christian, M. A., Gee, K. L., Wall, A. T., and Campbell, S. C. (**2024**). "Assessing impact of near-ground meteorology on spectral variability in static jet aircraft noise measurements," Proc. Mtgs. Acoust. **50**(1), 040010.
Sutherland, L. C. (**1993**). "Progress and problems in rocket noise prediction for ground facilities," in *15th AIAA Aeroacoustics Conference*, 25–27 October, Long Beach, CA, AIAA Paper 1993–4383.
Sutton, G. P., and Biblarz, O. (**2017**). *Rocket Propulsion Elements*, 9th ed. (Wiley, New York).
Tam, C., Golebiowski, M., and Seiner, J. (**1996**). "On the two components of turbulent mixing noise from supersonic jets," in *Aeroacoustics Conference*, 6–8 May, State College, PA, AIAA Paper 1996–1716.
United Launch Alliance (**2023**). "Vulcan Launch Systems User's Guide," available at https://www.ulalaunch.com/docs/default-source/default-document-library/2023_vulcan_user_guide.pdf?sfvrsn=37856b50_1 (Last viewed June 1, 2025).
United Launch Alliance (**2010**). "Atlas V Launch Services User's Guide," available at https://www.ulalaunch.com/docs/default-source/rockets/atlasvusersguide2010a.pdf?fvrsn=f84bb59e_2 (Last viewed June 1, 2025).
Varnier, J. (**2001**). "Experimental study and simulation of rocket engine freejet noise," AIAA J. **39**(10), 1851–1859.
Walter, U. (**2019**). *Astronautics: The Physics of Space Flight* (Springer, New York).
Ward, T. A. (**2010**). *Aerospace Propulsion Systems* (Wiley, New York).